JCI The Journal of Clinical Investigation

Cytokine therapy reverses NK cell anergy in MHC-deficient tumors

Michele Ardolino, Camillia S. Azimi, Alexandre Iannello, Troy N. Trevino, Lucas Horan, Lily Zhang, Weiwen Deng, Aaron M. Ring, Suzanne Fischer, K. Christopher Garcia, David H. Raulet

J Clin Invest. 2014;124(11):4781-4794. https://doi.org/10.1172/JCI74337.

Research Article

Various cytokines have been evaluated as potential anticancer drugs; however, most cytokine trials have shown relatively low efficacy. Here, we found that treatments with IL-12 and IL-18 or with a mutant form of IL-2 (the “superkine” called H9) provided substantial therapeutic benefit for mice specifically bearing MHC class I–deficient tumors, but these treatments were ineffective for mice with matched MHC class I^+ tumors. Cytokine efficacy was linked to the reversal of the anergic state of NK cells that specifically occurred in MHC class I–deficient tumors, but not MHC class I^+ tumors. NK cell anergy was accompanied by impaired early signal transduction and was locally imparted by the presence of MHC class I–deficient tumor cells, even when such cells were a minor population in a tumor mixture. These results demonstrate that MHC class I–deficient tumor cells can escape from the immune response by functionally inactivating NK cells, and suggest cytokine-based immunotherapy as a potential strategy for MHC class I–deficient tumors. These results suggest that such cytokine therapies would be optimized by stratification of patients. Moreover, our results suggest that such treatments may be highly beneficial in the context of therapies to enhance NK cell functions in cancer patients.

Cytokine therapy reverses NK cell anergy in MHC-deficient tumors

Michele Ardolino,[1] Camillia S. Azimi,[1] Alexandre Iannello,[1] Troy N. Trevino,[1] Lucas Horan,[1] Lily Zhang,[1] Weiwen Deng,[1] Aaron M. Ring,[2,3] Suzanne Fischer,[2,3] K. Christopher Garcia,[2,3] and David H. Raulet[1]

[1]Department of Molecular and Cell Biology, and Cancer Research Laboratory, Division of Immunology, University of California at Berkeley, Berkeley, California, USA. [2]Departments of Molecular and Cellular Physiology and Structural Biology, Stanford University School of Medicine, Stanford, California, USA. [3]Howard Hughes Medical Institute, Chevy Chase, Maryland, USA.

Various cytokines have been evaluated as potential anticancer drugs; however, most cytokine trials have shown relatively low efficacy. Here, we found that treatments with IL-12 and IL-18 or with a mutant form of IL-2 (the "superkine" called H9) provided substantial therapeutic benefit for mice specifically bearing MHC class I–deficient tumors, but these treatments were ineffective for mice with matched MHC class I$^+$ tumors. Cytokine efficacy was linked to the reversal of the anergic state of NK cells that specifically occurred in MHC class I–deficient tumors, but not MHC class I$^+$ tumors. NK cell anergy was accompanied by impaired early signal transduction and was locally imparted by the presence of MHC class I–deficient tumor cells, even when such cells were a minor population in a tumor mixture. These results demonstrate that MHC class I–deficient tumor cells can escape from the immune response by functionally inactivating NK cells, and suggest cytokine-based immunotherapy as a potential strategy for MHC class I–deficient tumors. These results suggest that such cytokine therapies would be optimized by stratification of patients. Moreover, our results suggest that such treatments may be highly beneficial in the context of therapies to enhance NK cell functions in cancer patients.

Introduction

Cytokines are powerful modulators of the immune system. Studies in mice have shown that cytokines can enhance the immune response to tumors (1) and opened the possibility of using them as immunotherapeutic agents. IL-2, for example, strongly activates T cells and NK cells. Clinical trials using high doses of IL-2 for advanced melanoma and renal carcinoma resulted in durable and complete responses, albeit in a small percentage (~5%) of patients and with substantial toxicity (2). IL-12 was notably efficacious in many murine tumor models (3–7), but provided responses in only 5% of patients with metastatic melanoma. A better understanding of the circumstances in which cytokine therapies are effective would provide an essential guide for future human clinical studies.

Many of the cytokines tested in clinical trials directly or indirectly activate natural killer (NK) cells. Several lines of evidence support a role for NK cells in antitumor immunity (8). The activation of NK cells is regulated by the integration of signals from activating and inhibitory cell surface receptors (9, 10). Inhibitory receptors specific for MHC class I molecules, including the Ly49 family members and the CD94/NKG2A heterodimer in mice, play a key role in this process. As a result of loss of inhibitory signals, target cells with low or no expression of MHC class I molecules become highly sensitive to killing by NK cells (9–11).

▶ Related Commentary: p. 4687

Conflict of interest: K. Christopher Garcia and Aaron M. Ring have filed a patent (US 2014/0046026 A1) describing the IL-2 "superkine" H9.
Submitted: November 18, 2013; **Accepted:** August 7, 2014.
Reference information: *J Clin Invest*. 2014;124(11):4781–4794. doi:10.1172/JCI74337.

Tumorigenesis is often accompanied by downregulation of MHC class I molecules (12), which should render the tumor cells sensitive to elimination by NK cells. The fact that many advanced tumor cells are deficient in MHC class I expression indicates that NK-mediated surveillance is often bypassed. However, the mechanisms underlying the escape of MHC class I–deficient tumor cells from NK cell–mediated immune surveillance are still unknown.

Here, we asked whether treatment with cytokines that activate NK cells provided therapeutic benefit in tumor-bearing mice by inducing activation of NK cells. We treated tumor-bearing mice with a combination of IL-12 and IL-18 or with an IL-2 mutant (H9 "superkine") capable of functioning independently of the α chain of the IL-2 receptor (13). Indeed, we observed that both treatments increased the survival of mice bearing MHC class I–deficient tumors, in an NK-dependent fashion. In contrast, cytokine treatment was completely ineffective in mice bearing matched tumors with high expression of MHC class I molecules. Notably, in the absence of cytokines, NK cells infiltrating MHC class I–deficient tumors acquired an anergic state, accounting for the failure of the cells to clear MHC class I–deficient tumor cells. The anergic state was similar to that of NK cells in MHC class I–deficient mice, and was associated with inefficient phosphorylation of signaling intermediates in activating pathways, and inefficient degranulation and cytokine production after stimulation. Tumor cells with restored MHC class I expression failed to induce anergy. Importantly, the cytokine treatments, in addition to improving survival, reversed the anergy of NK cells within the tumors. Altogether, these results support a model in which NK cells infiltrating MHC class I–deficient tumors are reset to an anergic state, which can be reversed by inflammatory cytokines, resulting in therapeutic benefit.

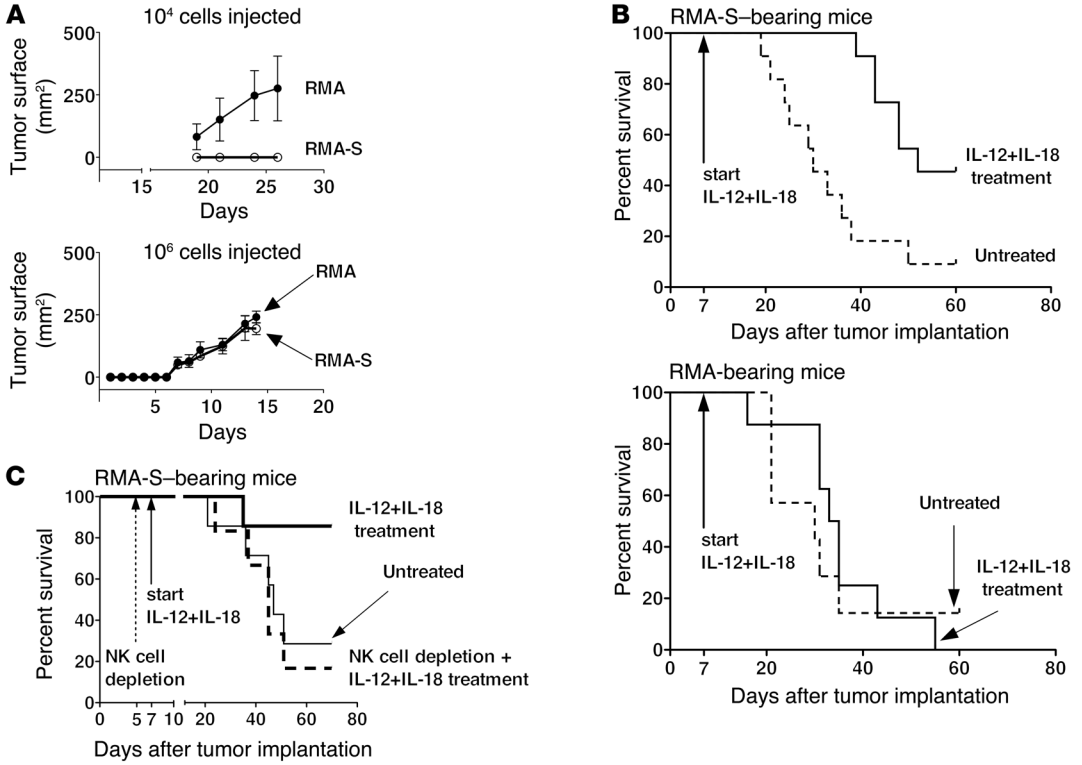

Figure 1. IL-12+IL-18 treatment increases survival of mice bearing MHC class I–deficient tumors. (**A**) 10^4 or 10^6 RMA or RMA-S cells were injected s.c. in B6 mice. Tumor growth was assessed by caliper measurement. (**B** and **C**) Kaplan-Meier analyses of RMA-S– or RMA-bearing mice treated or not with 100 ng each of IL-12+IL-18 every other day starting 7 days after implanting 10^6 tumor cells. In **C**, 1 group of mice was depleted of NK cells by a weekly i.p. injection of 200 μg of PK136 antibody, starting 5 days after implantation of tumor cells. NK depletion of the cytokine-treated group resulted in significantly reduced survival ($P = 0.02$) according to the log-rank (Mantel-Cox) test. The experiments included at least 4 mice per group and were performed at least 2 times with similar results.

Results

Treatment with NK cell–activating cytokines improves the survival of mice bearing MHC class I–deficient tumors, in an NK cell–dependent fashion. Cellular transformation is often accompanied by reduced expression of MHC class I molecules (12). In order to characterize why MHC class I–deficient tumor cells are not cleared in vivo, we took advantage of RMA-S cells, a C57BL/6 (B6) T cell lymphoma cell line with low MHC class I expression, generated by mutagenesis and selection of the parental cell line RMA (14–16). When implanted s.c. into B6 mice, 10^4 RMA-S cells were rejected, in an NK-dependent fashion (refs. 15, 16, and Figure 1A, top panel). However, a higher dose of RMA-S cells (10^6) resulted in tumor progression in many or all of the mice, virtually identical to the results obtained with the same dose of RMA cells (Figure 1A, bottom panel).

Cytokine treatment has been used in studies of tumor rejection in mice before, but it has not been specifically examined whether the efficacy of cytokine treatments was related to MHC class I expression by tumor cells. To determine whether injection of IL-12 and IL-18 was beneficial in the context of MHC class I–deficient tumor cells, we initiated tumors and commenced cytokine treatments 7 days later. Notably, cytokine treatment of RMA-S–bearing mice resulted in a significantly prolonged average survival time, and a higher fraction of mice that survived long term (the survivors at day 60 had no detectable tumors) (Figure 1B, top panel). The benefit of the cytokine treatment in mice with RMA-S tumors was completely abrogated if the mice were NK-depleted, demonstrating that the effect of the cytokines depended on NK cells (Figure 1C).

The efficacy of cytokine treatments in mice bearing RMA-S tumors did not apply to mice bearing RMA tumors, which are similar to RMA-S cells except that they express high amounts of MHC class I and are therefore resistant to NK cells (Figure 1B, bottom panel). The survival time in mice with RMA tumors did not change when the mice were treated with cytokines, and was similarly rapid to that in untreated mice with RMA-S tumors.

Recently, Levin and colleagues described the "superkine" H9, an engineered version of IL-2, which functions independently of the α chain (CD25) of the IL-2 receptor. Compared with WT IL-2, H9 exhibits much more activity on NK cells and T cells. In vivo, H9 stimulated rejection of B16F10 melanoma tumors in B6 mice (13), but the role of NK cells in rejection has not been investigated. We tested whether H9 induces NK-dependent rejection of MHC class I–deficient tumors by implanting high doses of RMA-S or RMA cells and initiating H9 treatment after 7 days. Similar to the results with IL-12+IL-18 treatment, H9 resulted in improved survival of RMA-S–bearing mice, but had no effect in RMA-bearing mice (Figure 2, A and B). Notably, when mice were depleted of NK cells, the efficacy of H9 treatment was abolished (Figure 2A). These results show that H9 exerts its antitumor effect against MHC class I–deficient tumor cells in an NK cell–dependent fash-

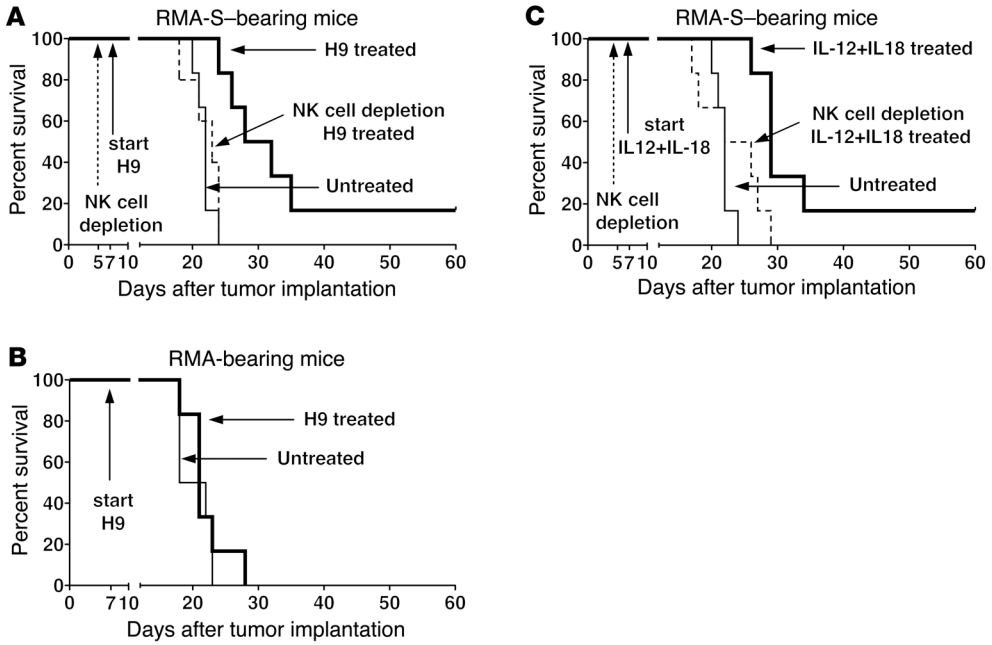

Figure 2. Treatment with IL-2 mutant H9 superkine increases survival of RMA-S–bearing mice in an NK-dependent fashion. 10^6 RMA-S or RMA cells were injected s.c. in B6 mice. In **A** and **C,** a group of mice were depleted of NK cells by a weekly i.p. injection of 200 μg of PK136 antibody, starting 5 days after implantation of tumor cells. In **A** and **B**, mice were treated with 20 μg of H9 every other day starting 7 days after tumor implantation, whereas in **C**, mice were treated with 100 ng each of IL-12+IL-18 every other day starting 7 days after tumor implantation. The "Untreated" group is shared by **A** and **C**. The log-rank (Mantel-Cox) test was used to compare: in **A**, Untreated versus H9-treated mice ($P = 0.002$); in **B**, Untreated versus H9-treated mice (NS); and in **C**, Untreated versus IL-12+IL-18–treated mice ($P = 0.001$). The experiments included at least 5 mice per group and were performed 4 times with similar results.

ion. Together, these data showed that both IL-12+IL-18 and H9 were beneficial in the context of MHC class I–deficient RMA-S tumors but not in the case of MHC class I^+ RMA tumors.

Growth of MHC class I–deficient tumors is associated with induction of functional anergy in tumor-infiltrating NK cells. The growth of tumors when mice were challenged with a high dose of RMA-S cells in the absence of cytokines suggested a failure of NK cell–mediated surveillance of MHC class I–deficient cells in this context. One possibility to explain the results was that NK cells were somehow excluded from such tumors. However, we found a similar number of NK cells within RMA-S and RMA tumors (Figure 3A), excluding this possibility. Furthermore, there were no significant differences in the viability of NK cells within the 2 types of tumors (data not shown). These results, and the evidence that activating cytokines induced NK cell–mediated elimination of MHC class I–deficient tumors, led us to hypothesize that NK cells in the tumor bed must be ineffective or functionally impaired with respect to eliminating the MHC class I–deficient tumor cells.

Previous reports showed that NK cells acquire a functionally anergic phenotype in MHC class I–deficient mice in steady-state conditions (17). To test whether MHC class I–deficient tumor cells induced functional anergy in tumor-infiltrating NK cells, B6 mice were challenged with a high dose of RMA or RMA-S tumor cells, and NK cell responsiveness was analyzed ex vivo 14 days later. Responsiveness was assayed by stimulation of NK cells with plate-bound antibody specific for the activating receptor NKR-P1C, followed by flow cytometry to assess intracellular IFN-γ production and/or degranulation (indicated by CD107a expression) (18, 19). Notably, NK cells infiltrating MHC class I–deficient RMA-S tumors responded poorly compared with those infiltrating RMA tumors in both the degranulation and cytokine production assays (Figure 3, B and C, and data not shown). The anergic state of these NK cells may therefore account for their inability to reject the MHC class I–deficient tumors.

Deficiency of MHC class I expression in RMA-S cells is the result of a mutation in the *Tap2* gene (15, 20, 21). Therefore, we tested whether anergy in RMA-S–infiltrating NK cells was due to the absence of MHC class I on tumor cells, rather than some other acquired distinctive features of these long-separated cell lines. RMA-S cells were transduced with WT *Tap2*, resulting in high MHC class I expression, comparable to that of RMA cells (not shown). Notably, NK cells infiltrating RMA-S/*Tap2* tumors exhibited high functional activity similar to that of NK cells infiltrating RMA tumors (Figure 3D). These results represented definitive evidence that the absence of MHC class I on RMA-S cells caused the anergic state in tumor-infiltrating NK cells.

To establish the kinetics of NK cell anergy induction in the tumor bed, we analyzed the responsiveness of infiltrating NK cells 7, 10, and 14 days after tumor cell injection. To facilitate analysis of small developing tumors at the earlier time points, tumor cells were injected in combination with Matrigel (22), which provides a support for tumor establishment. Interestingly, NK cells infiltrating RMA-S–derived tumors were anergic after only 7 days (Figure 3E), suggesting that NK cell anergy induction occurred relatively early in tumor development. Altogether, these results show that in immunocompetent mice the growth of MHC class I–deficient tumors is associated with the induction of functional anergy of infiltrating NK cells.

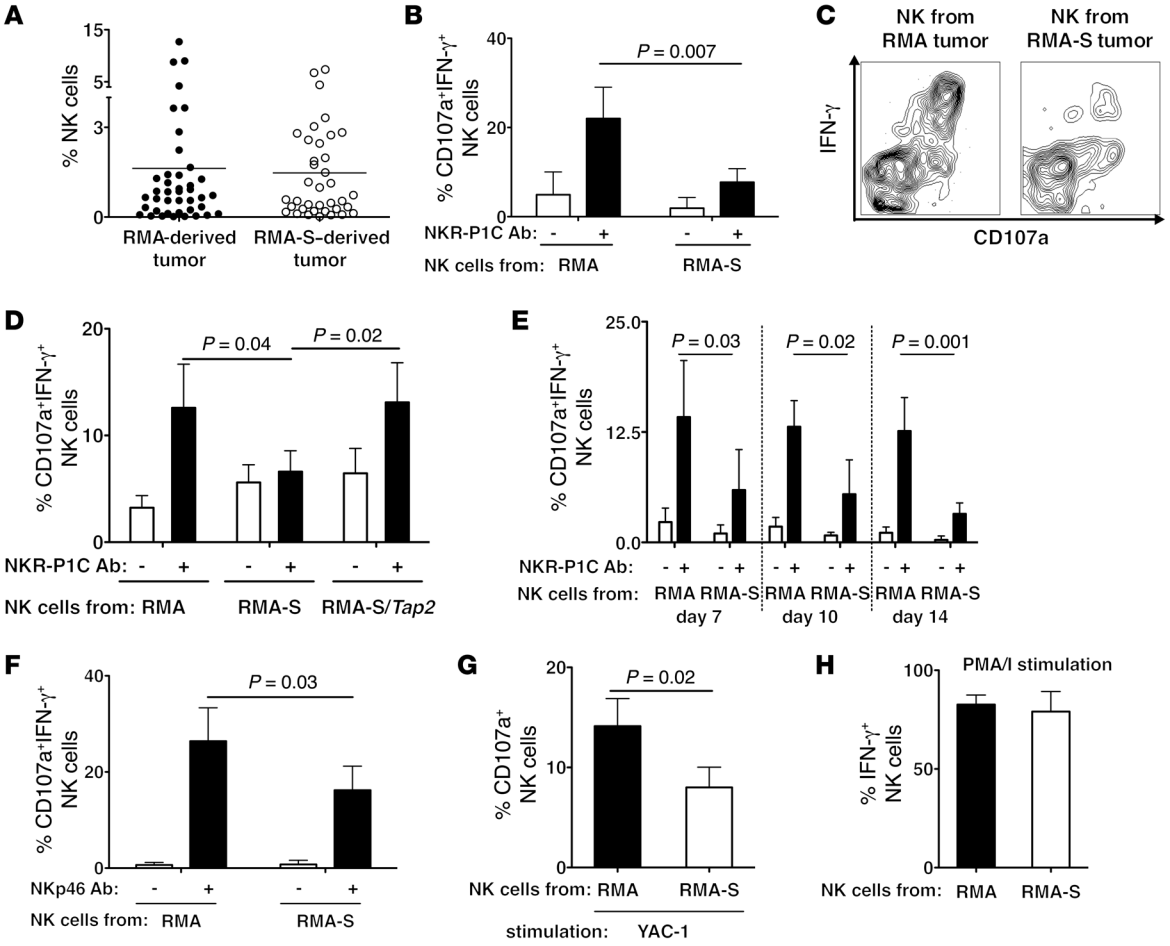

Figure 3. NK cells infiltrating MHC class I–deficient tumors have impaired functional responsiveness. (**A**–**C**) Fourteen days after implantation, the percentages of NK cells among the viable cells in the tumors (**A**) and their responsiveness (**B** and **C**) were assessed by flow cytometry. Infiltrating leukocytes were restimulated in vitro with NKR-P1C antibody or control IgG (indicated as "+" and "–" in the legends), and IFN-γ accumulation and/or CD107a expression were determined. (**D**) Functional responsiveness of NK cells infiltrating tumors derived from RMA, RMA-S, or RMA-S/*Tap2* cells was assayed as described in **A**. (**E**) RMA or RMA-S cells were injected in a Matrigel solution 7, 10, or 14 days before the functional assays were performed. (**F**) Tumor-infiltrating leukocytes were restimulated in vitro with NKp46 antibody or control IgG, and IFN-γ accumulation and CD107a expression were evaluated. (**G**) RMA or RMA-S cells were implanted in Ubi-GFP/BL6 hosts, and after 14 days tumor-infiltrating leukocytes were sorted and cocultured for 5 hours with YAC-1 cells at an effector/target ratio of 10:1. NK cell degranulation was determined by assaying of CD107a expression at the cell surface. (**H**) Leukocytes from RMA or RMA-S tumors were stimulated with PMA and ionomycin before IFN-γ accumulation on NK cells was measured by flow cytometry. In all graphs, bars represent means ± SD. In all panels NK cells were gated as viable-$CD3^-CD19^-Ter119^-NKp46^+$ cells. The experiments included at least 4 mice per group and were performed 10 (**B**), 3 (**D** and **F**), or 2 (**E**, **G**, and **H**) times with similar results. Statistical analyses were performed with the 2-tailed unpaired Student's *t* test.

Since NKR-P1C is one of several NK-activating receptors, we analyzed whether the functional impairment of NK cells in MHC class I–deficient tumors extended to other activating receptors. Stimulation of tumor-infiltrating NK cells with plate-bound NKp46 antibody recapitulated the results with NKR-P1C antibody: the NK cells infiltrating MHC class I–deficient tumors were anergic compared with NK cells in RMA tumors (Figure 3F).

To determine whether NK cells infiltrating MHC class I–deficient tumors were hyporesponsive to stimulation with unrelated tumor cells, we implanted RMA or RMA-S tumors into mice ubiquitously expressing GFP (Ubi-GFP/BL6) (23). After 14 days, we sorted tumor-infiltrating leukocytes and stimulated them with NK-sensitive YAC-1 tumor cells. Notably, NK cells infiltrating MHC class I–deficient tumors exhibited a reduced degranulation response after YAC-1 stimulation (Figure 3G). Hence, the impaired in vitro responses to antibody stimulation and tumor cells recapitulated the defective rejection response observed in vivo. This desensitization of NK cells likely accounts for the escape of the RMA-S tumors from NK surveillance.

Interestingly, NK cells from MHC class I–deficient tumors were fully responsive to stimulation with PMA plus ionomycin, pharmacological activators that bypass early receptor signaling events (Figure 3H). These data suggested that the anergy of NK cells in MHC class I–deficient tumors reflects impaired early signaling events in the receptor activation pathway. NK cells from MHC class I–deficient mice, which are also anergic, were also hyporesponsive to stimulatory antibodies but normally responsive to PMA plus ionomycin (18).

To demonstrate the generality of our findings we sought to test an additional MHC class I–deficient tumor model. In order to generate an MHC class I–deficient tumor cell line that could

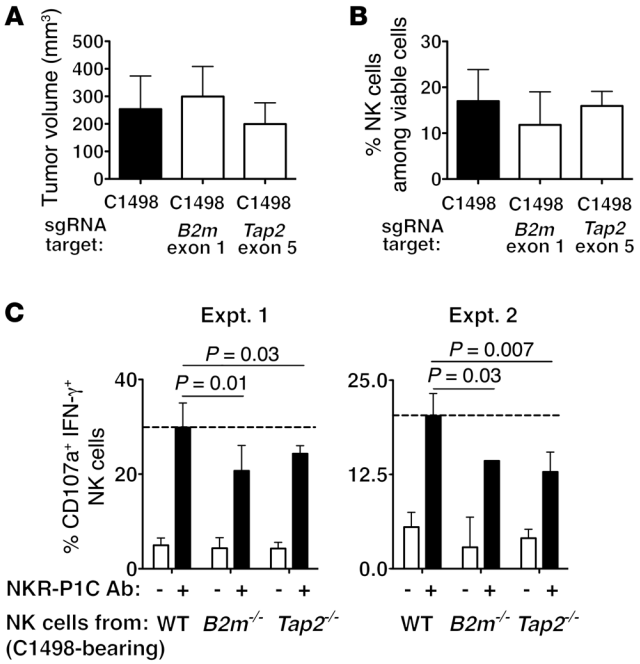

Figure 4. Anergy of NK cells infiltrating MHC class I–deficient mutants of the C1498 cell line. C1498, C1498-*B2m*, and C1498-*Tap2* cells were implanted s.c. into B6 mice. After 14 days, tumor volume was measured (**A**), and NK cell infiltration (**B**) and responsiveness (**C**) were assessed as described in the legend to Figure 3. In **C**, 2 independent experiments are shown. Bars represent means ± SD. NK cells were gated as in Figure 3. The experiments included at least 5 mice per group. Statistical analyses were performed with the 2-tailed unpaired Student's *t* test.

be compared with an MHC class I$^+$ counterpart, we used the CRISPR/Cas9 system (24, 25) to knock out the *B2m* or the *Tap2* gene in the B6-derived C1498 cell line (26). Once the cell lines were generated and loss of MHC class I was corroborated by flow cytometry, we compared C1498 cells with C1498-*B2m*$^{-/-}$ and C1498-*Tap2*$^{-/-}$ cell lines in vivo. Using a high dose of tumor cells, the MHC class I–deficient C1498 tumors grew to dimensions similar to those of WT C1498 tumors (Figure 4A), whereas with lower doses, only the WT tumor cells grew (data not shown). As also observed in the RMA/RMA-S system, the MHC class I–deficient C1498 tumors contained similar numbers of NK cells to the MHC class I$^+$ C1498 tumors (Figure 4B). Most importantly, the NK cells in the tumor bed of the MHC class I–deficient C1498 tumors were functionally anergic compared with the NK cells in C1498 tumors, although to a lower extent than was observed in the RMA/RMA-S system (Figure 4C). These results showed the generality of the conclusion that in vivo growth of MHC class I–deficient tumors is associated with NK cell anergy.

Anergic tumor-infiltrating NK cells exhibit impaired signal transduction in response to stimulation. The results presented above suggested that NK cell anergy was associated with impaired early signaling events. A similar functional anergy was observed in MHC class I–deficient mice (10, 19, 27, 28), but the molecular mechanisms behind it have not been elucidated.

The anergy of WT NK cells in MHC class I–deficient tumors may be mechanistically similar to the anergy of NK cells that fail to encounter MHC class I in steady-state conditions, such as in MHC class I–deficient mice or in WT NK cells transferred to MHC class I–deficient mice (17, 18). To determine whether specific signaling pathways were impaired in anergic NK cells, we examined signal transduction resulting from aggregation of activating receptors ex vivo. ERK1/2 kinase is important for promoting cytotoxicity and cytokine secretion by NK cells (29, 30), so we initially tested ERK1/2 phosphorylation in freshly isolated NK cells from WT versus MHC class I–deficient mice, after in vitro stimulation with NKR-P1C antibody. As detected by Western blotting and intracellular staining with an antibody specific for the T202/Y204-phospho-ERK1/2 (31), ERK activation was significantly reduced in MHC class I–deficient NK cells as compared with WT NK cells, despite similar ERK levels (Figure 5, A and B). These data suggest that NK cell anergy in MHC class I–deficient mice is imposed by mechanisms that dampen signaling upstream of ERK1/2 activation. Notably, WT NK cells infiltrating MHC class I–deficient tumors exhibited a similar defect in ERK1/2 phosphorylation compared with WT NK cells infiltrating RMA tumors (Figure 5, C and D). These data support the conclusion that anergy of NK cells in RMA-S tumors is mechanistically similar to the anergy of NK cells in MHC class I–deficient mice. Similarly, phosphorylation of AKT on S473 was also reduced in the NK cells infiltrating MHC class I–deficient tumors, although to a lesser extent (Figure 5, E and F). These results show that the anergic state in NK cells is associated with reduced intracellular transmission of activating signals from activating cell surface receptors.

NK cell anergy is restricted to the tumor proximal environment. The induction of NK cell anergy described so far is a new mechanism by which MHC class I–deficient tumor cells escape from NK cell immunosurveillance. To address whether NK cell anergy in RMA-S tumors was induced locally or systemically, we injected RMA or RMA-S cells in 2 different flanks of the same mice, and assessed the responsiveness of NK cells infiltrating the 2 types of tumors. In the experiments shown in Figure 6, unlike some others, RMA-S tumors had smaller average sizes than RMA tumors when injected in different mice or in the same mice, but the differences were not statistically significant in either case (Figure 6A). NK cells infiltrating MHC class I–deficient tumors were less responsive than NK cells in RMA tumors, even when the 2 types of tumors were implanted in the same mice (Figure 6B and not shown). These results demonstrate that NK cell anergy is pronounced in the local environment but less so in a distant MHC class I$^+$ tumor.

To corroborate and extend these results, we analyzed NK responsiveness in tumor-draining and nondraining lymph nodes of mice that received RMA or RMA-S tumors. Interestingly, NK cells resident in the lymph nodes draining MHC class I–deficient tumors were substantially less responsive than NK cells in lymph nodes draining MHC class I$^+$ tumors. In contrast, NK cells in distant lymph nodes, or in the spleen, responded more similarly in mice bearing MHC class I–deficient and MHC class I$^+$ tumors (Figure 6, C–E). Even after normalization and combining of the results of 5 experiments, the responsiveness of NK cells in distant lymph nodes or spleens of RMA versus RMA-S tumors did not differ significantly, whereas the NK cells in the draining lymph nodes differed very significantly ($P = 3 \times 10^{-7}$).

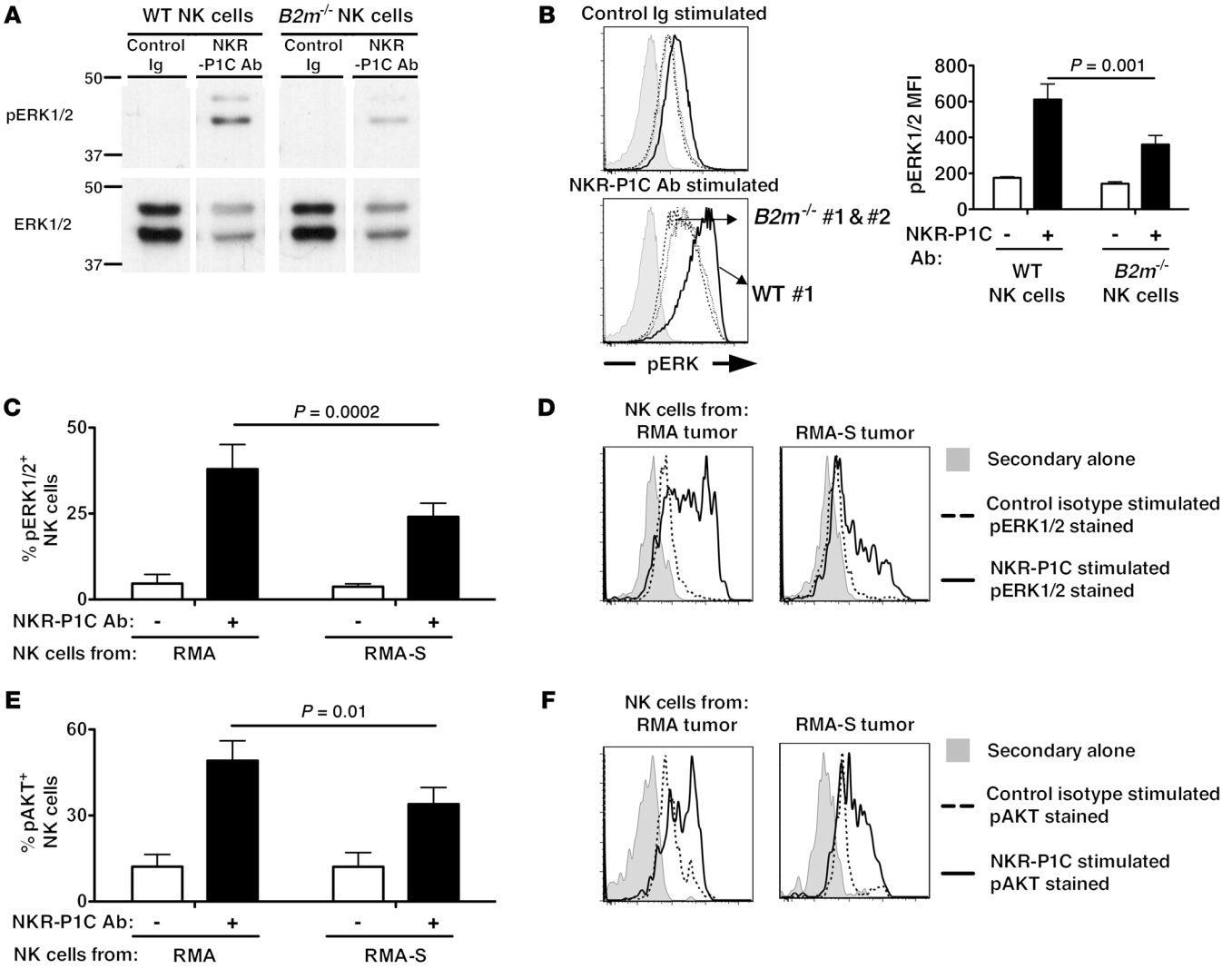

Figure 5. NK cells infiltrating MHC class I–deficient tumors exhibit impaired signaling downstream of activating receptors. (**A**) Splenic NK cells were sorted from WT or *B2m*$^{-/-}$*Ncr1*$^{+/GFP}$ mice and stimulated with NKR-P1C mAb or control IgG for 30 minutes. Western blot analysis was performed on cell lysates using a pERK1/2 mAb. Total ERK1/2 was used as a control. The samples were run on the same gel. The apparent difference in total ERK1/2 amounts between unstimulated and stimulated samples was due to unequal loading of the samples (data not shown). (**B**) Splenic cells from WT or *B2m*$^{-/-}$ *Ncr1*$^{+/gfp}$ mice were stimulated with NKR-P1C mAb or control IgG for 3 minutes, and pERK1/2 levels on NK cells were analyzed by intracellular staining. (**C**–**F**) *Ncr1*$^{+/gfp}$ mice were injected with RMA or RMA-S cells, and after 14 days, tumor-infiltrating leukocytes were stimulated with NKR-P1C mAb or control IgG as in **B**. Cells were then fixed and stained for pERK1/2 (**C** and **D**) or pAKT (**E** and **F**). The pERK and pAKT profiles of tumor-derived NK samples were somewhat erratic because of the analysis of relatively few NK cells (~1,000) per sample, but comparing numerous animals, the differences were highly significant. (**B**–**F**) NK cells were identified by GFP expression. Bars represent means ± SD. The experiments included at least 4 mice per group and were performed 2 (**A**), 3 (**B**), or 4 (**C**–**F**) times with similar results. Statistical analyses were performed with the unpaired Student's *t* test.

Notably, a small population of RMA-S tumor cells was detected within the tumor-draining lymph nodes, but not within the distant lymph nodes or in the spleen (Figure 6F and not shown). These data show that NK cell anergy is imparted locally rather than systemically, possibly thorough sustained interaction between NK cells and MHC class I–deficient tumor cells. Note that NK cells in lymph nodes draining either RMA or RMA-S tumors were consistently, though only slightly, more responsive than the NK cells in distant lymph nodes, possibly because of stimulatory effects of the local tumor environment (Figure 6C vs. Figure 6D). Taken together, these results show that NK cell anergy is imparted locally by MHC class I–deficient tumor cells in the tumor bed and in the draining lymph nodes.

NK cell anergy is not correlated with altered expression of surface markers, proliferation, or suppressive cells or cytokines. NK cells are heterogeneous with respect to receptor expression, and different NK subsets vary in their responsiveness (32). Among mature (CD11b^{+}) NK cells, those expressing inhibitory receptors for self MHC class I molecules (Ly49C, Ly49I, and CD94/NKG2A in B6 mice) are the most responsive (18, 33). To determine whether NK cell anergy in MHC class I–deficient tumors was associated with an immature phenotype or with lack of self MHC class I–specific inhibitory receptors, we determined the phenotypes of NK cells infiltrating RMA and RMA-S tumors. We observed a similar distribution of the 2 mature subsets (CD11b^{+}CD27^{+} and CD11b^{+}CD27^{-} cells) (Fig-

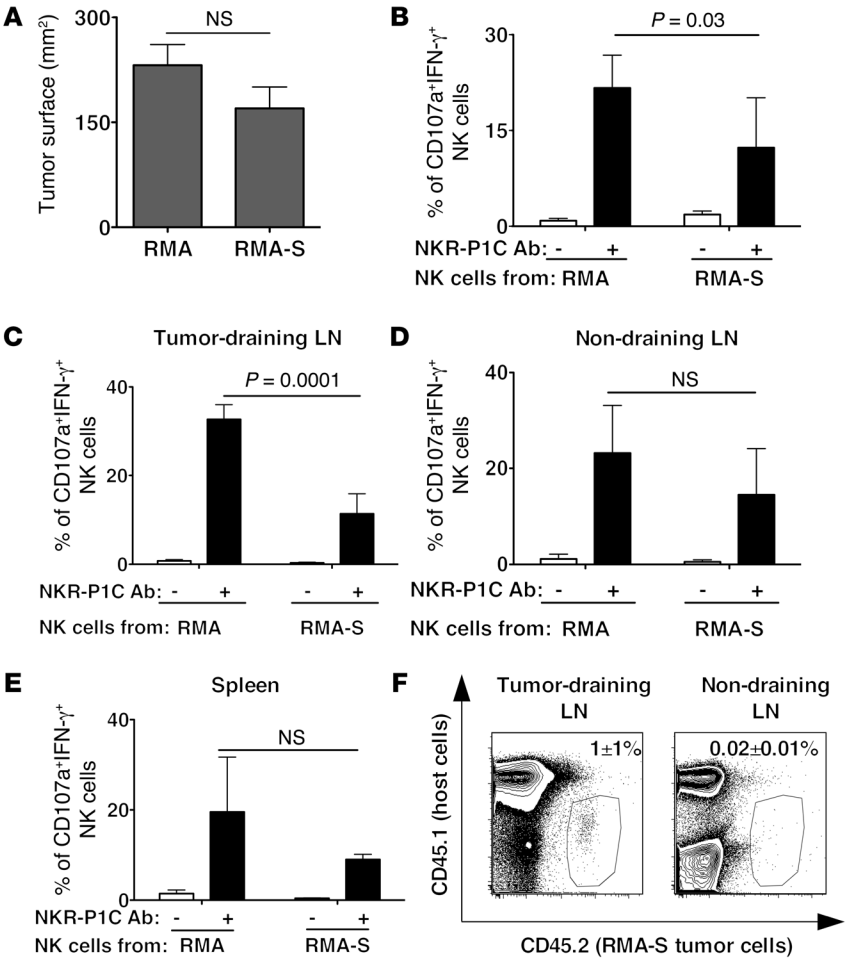

Figure 6. NK cell anergy is locally induced and requires close proximity with MHC class I–deficient tumor cells. (**A** and **B**) RMA or RMA-S cells were injected in 2 different flanks of the same mice, and tumor size (**A**) and NK cell responsiveness (**B**) were evaluated at day 14. (**C**–**E**) Responsiveness of NK cells from tumor-draining or nondraining lymph nodes or the spleen was determined as described in the legend to Figure 3. Bars represent means ± SD. (**F**) RMA-S tumor cells (CD45.2$^+$) were injected in B6-CD45.1$^+$ mice, and after 14 days the content of tumor cells in the tumor-draining or nondraining lymph nodes was determined. Two representative plots are depicted, while the percentages in the plots represent means ± SD of 3 independent experiments with $n = 9$ total. NK cells were gated as described above. The experiments included at least 4 mice per group and were performed 2 (**A** and **B**) or 3 (**C**–**F**) times with similar results. Statistical analyses were performed with the 2-tailed unpaired Student's *t* test, except for **B**, where a 2-tailed paired Student's *t* test was used.

ure 7A and Supplemental Figure 1A; supplemental material available online with this article; doi:10.1172/JCI74337DS1). Furthermore, there were no differences in the percentages of NK cells expressing inhibitory receptors specific for self MHC class I (Ly49C, Ly49I, and NKG2A), nor in the percentages of cells expressing Ly49G2 or Ly49A (Figure 7B and Supplemental Figure 1B). Finally, we observed no differences in the expression of activating receptors such as NKR-P1C, NKp46, DNAM-1, and NKG2D (Figure 7C).

We further tested whether the lower responsiveness of NK cells in MHC class I–deficient tumors was associated with an increased recruitment of CD4$^+$ Tregs or myeloid-derived suppressor cells (MDSCs), both capable of inhibiting NK cell responses (34–38). Notably, in the 2 types of tumors the ratios of Tregs to NK cells, and MDSCs to NK cells, were similar (Figure 7, D and E). Similar results were obtained in multiple repetitions of the experiment (Supplemental Figure 2). Moreover, no differences were observed even when the data were analyzed in terms of the absolute numbers or percentages of Tregs and MDSCs in the tumors (not shown). Finally, further analyses showed that F4/80-positive MDSCs or Ly6G-positive MDSCs were also similarly represented within RMA versus RMA-S tumors (data not shown).

NK cells undergoing homeostatic proliferation after transfer to tumor-bearing mice become exhausted and fail to reject the tumor (39). However, the proliferative status of NK cells in RMA and RMA-S tumors was very similar as assessed by Ki67 staining ex vivo, arguing that differential proliferation did not account for the different responsiveness (Figure 7F).

Finally, we determined whether the reduced NK responsiveness in RMA-S tumors was associated with increased expression of immune-suppressive cytokines such as TGF-β or IL-10. However, TGF-β1 transcripts were present at similar levels in the RMA and RMA-S tumors (Figure 7G), and similar amounts of active TGF-β1 were detected by ELISA in RMA and RMA-S tumors or in the sera of mice bearing these tumors (Supplemental Figure 3). Furthermore, we failed to detect TGF-β2 or TGF-β3 transcripts in RMA or RMA-S tumors, arguing against a role for these isoforms of the cytokine in imposing anergy (data not shown). Finally, we also observed no differences in the amount of IL-10 transcripts in RMA and RMA-S tumors (not shown). Together, these data suggest that neither TGF-β nor IL-10 accounts for anergy of NK cells in RMA-S tumors.

These results failed to correlate anergy of NK cells in MHC class I–deficient tumors with NK immaturity, differential expression of inhibitory receptors, markers of proliferation, or the presence of inhibitory cells or cytokines. We propose instead that the NK cells are rendered anergic by other cell-intrinsic mechanisms resulting from sustained stimulation from MHC class I–deficient tumor cells such as the aforementioned impairment in early steps of stimulatory receptor signal transduction.

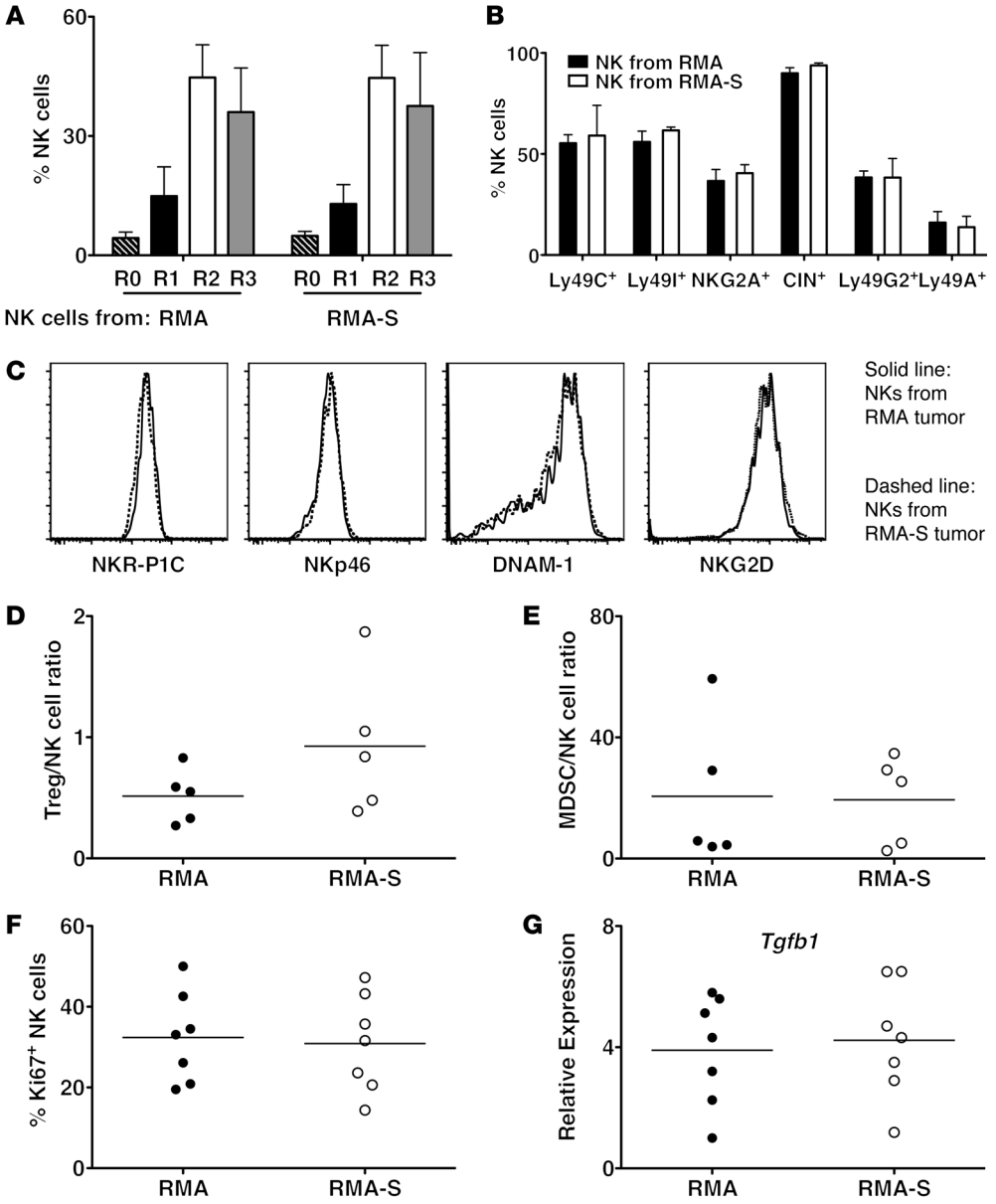

Figure 7. NK cell anergy in MHC class I–deficient tumor-bearing mice is not associated with alterations in NK cell subpopulations, increased recruitment of immune-infiltrating cells, increased proliferation, or differences in the inflammatory environment. (**A** and **B**) NK cells from RMA or RMA-S tumors were stained with antibodies for CD27 and CD11b to identify the R0–R3 stages (R0 = $CD27^-CD11b^-$; R1 = $CD27^+CD11b^-$; R2 = $CD27^+CD11b^+$; R3 = $CD27^-CD11b^+$) or for the inhibitory receptors Ly49C, Ly49I, NKG2A, Ly49G, and Ly49A. "CIN^+" in the graph indicates NK cells expressing at least 1 of the 3 receptors Ly49C, Ly49I, and NKG2A. Bars represent means ± SD. (**C**) NK cells from RMA or RMA-S tumors were stained for NKp46, NKR-P1C, DNAM-1, and NKG2D. Representative histograms are shown. (**D** and **E**) Ratios of Tregs or MDSCs to NK cells were calculated in RMA- or RMA-S–derived tumors. NK cells were gated as viable-$CD3^-CD19^-Ter119^-NKp46^+$ cells. Tregs were gated as viable-$CD19^-Ter119^-NKp46^-CD3^+CD4^+Foxp3^+$ cells, and MDSCs were gated as viable-$CD3^-CD19^-Ter119^-NKp46^-CD11b^+$ cells. (**F**) Proliferation status of NK cells infiltrating RMA or RMA-S tumors was assessed by Ki67 staining. (**G**) Relative expression of *Tgfb1* mRNA was determined by quantitative PCR in RNA prepared from whole tumor lysates. The experiments included at least 4 mice per group and were performed 3 (**A**, **B**, and **D**–**G**) or 2 (**C**) times with similar results. Statistical analyses were performed with the 2-tailed unpaired Student's *t* test.

Loss of MHC class I expression on a portion of tumor cells is sufficient to disarm the infiltrating NK cells. Loss of MHC class I by tumors under natural conditions likely occurs progressively, as a few cells with mutations causing MHC class I deficiency are enriched because of selective elimination of MHC class I^+ tumor cells. It was therefore of interest to assess whether anergy occurs in a mixed environment, where only a fraction of the cells are MHC class I–deficient. To mimic this situation, we injected mice with RMA, RMA-S, or mixtures of the 2 cell lines (10^6 total) in proportions ranging from 0.5:1 to 2:1. The sizes of the resulting tumors were in a similar range whether RMA and RMA-S cells were injected separately or in mixtures (Figure 8A). Although we always detected some RMA-S cells in the tumors arising from the mixtures, in all circumstances the majority of cells were RMA cells (Figure 8B), suggesting that some but not all of the RMA-S cells in the mixtures were eliminated. Importantly, NK cells in the mixed MHC class I tumor environment in all cases exhibited a state of anergy similar to that of NK cells in fully RMA-S tumors (Figure 8C), indicating that even a minority of MHC class I–deficient tumor cells can dominantly impose anergy of the infiltrating NK population.

Cytokines reverse the functional anergy of NK cells. Treatments with IL-12 and IL-18 had a dramatic effect on the survival of mice bearing MHC class I–deficient tumors (Figures 1 And 2). Since we found that the growth of such tumors was associated with the induction of NK cell anergy, we wondered whether the effectiveness of cytokine treatments was due to a reversion of the anergic state.

Initially, we tested whether NK cells extracted from MHC class I–deficient tumors responded differentially to the activating cytokines. We therefore stimulated NK cells from RMA or RMA-S tumors with 2 doses of IL-12 and IL-18 and assessed IFN-γ production by the cells. The results showed a nearly identical response from NK cells infiltrating RMA-S and RMA tumors (Figure 9A), ruling out the possibility that the different tumor rejection responses were due to desensitization of IL-12 and IL-18

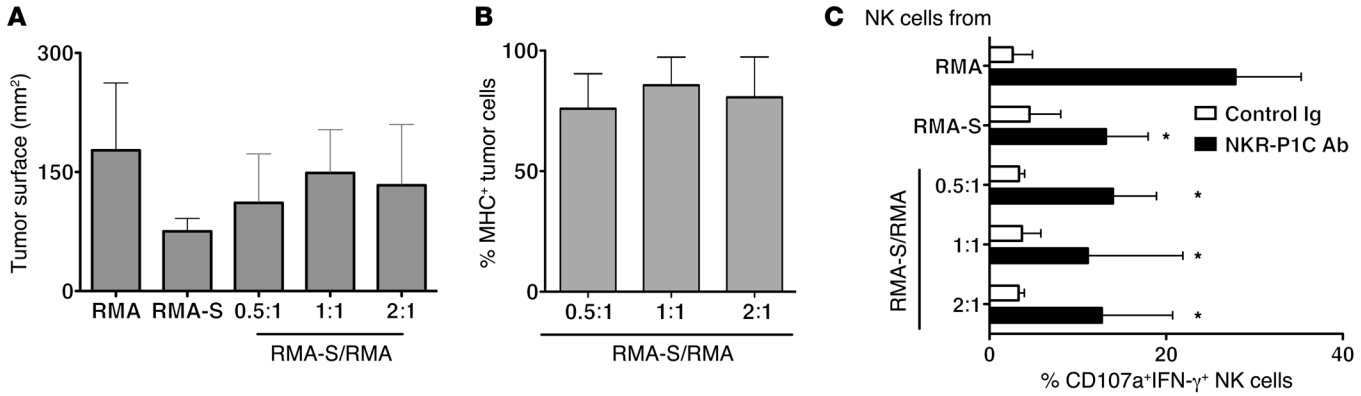

Figure 8. A minor fraction of MHC class I–deficient tumor cells dominantly induces NK cell anergy. Mice were injected with RMA, RMA-S, or mixtures of the 2 cell lines at the ratios shown. After 14 days, tumor sizes (**A**) were evaluated by caliper measurements. The ratios between RMA and RMA-S in the tumors (**B**) were determined by analysis of MHC class I expression on tumor cells. NK cell responsiveness (**C**) was determined as described in the legend to Figure 3. The experiments included at least 4 mice per group and were performed 2 times with similar results. Bars represent means ± SD. Statistical analyses were performed with the 2-tailed unpaired Student's *t* test. $^*P < 0.05$ with respect to RMA group.

receptors. Consistent with the functional results, anergic NK cells, both from *B2m*-deficient mice (Figure 9B) and in the bed of RMA-S tumors (Figure 9C), did not exhibit impaired ERK1/2 phosphorylation levels in response to IL-12+IL-18 stimulation. Importantly, similar results were obtained by stimulation of WT (responsive) and *B2m*-deficient (anergic) NK cells with both IL-2 and the H9 "superkine" (Figure 9D). As predicted on the basis of a previous study (13), ERK phosphorylation in NK cells occurred with much lower doses of H9 than of IL-2 (Figure 9D). These results showed that anergic NK cells from MHC class I–deficient tumors or MHC class I–deficient mice exhibit normal functional responses and ERK phosphorylation responses when stimulated with cytokines, including IL-12+IL-18, H9, or IL-2. Hence, although these NK cells are anergic to stimulation through cell surface activating receptors, they are not anergic to stimulation by these cytokines, and anergy cannot be explained by a defective response to these cytokines. Interestingly, we found little or no *Il12* or *Il18* mRNA in preparations of total RNA from either RMA- or RMA-S–derived tumors (data not shown), arguing that these cytokines are not normally produced in significant quantities in these tumors.

Having shown that anergic NK cells respond as well as nonanergic NK cells to cytokine stimulation, we next determined whether treatments with IL-12 and IL-18 in vivo revert the NK cell anergic phenotype. Mice were challenged with RMA-S cells and 13 days later were injected with IL-12 and IL-18, and the responsiveness of tumor-infiltrating NK cells was tested 24 hours later. Compared with tumor-infiltrating NK cells from untreated mice, tumor-infiltrating NK cells from the cytokine-treated mice exhibited substantially elevated responses to NKR-P1C stimulation, over a somewhat elevated background response (Figure 9E). The NK cells from IL-12+IL-18–treated mice also significantly upregulated CD25 expression (Figure 9F), which has previously been shown to enable NK cells to proliferate in response to IL-2 (40).

Taken together, these results show that NK cell anergy is induced as a result of persistent stimulation by the MHC class I–deficient tumor cells in the absence of an activating inflammatory environment. Although some of the MHC class I–deficient tumor cells may initially be killed, as suggested by the experiments with mixed RMA/RMA-S tumors, the eventual induction of anergy enables the tumors to escape from NK cell immune surveillance. However, treatment with proinflammatory cytokines reversed the anergic NK cell phenotype, providing therapeutic benefit to animals with MHC class I–deficient tumors.

Discussion

Cancer immunotherapy research has met with numerous recent accomplishments, such as the successful clinical trials with antibodies that target immunosuppressive molecules such as CTLA-4 and PD-1 (41). Earlier attempts to treat cancer with activating cytokines provided excellent results in some preclinical systems but yielded disappointing results in human trials in two respects: (a) the treatments were often highly toxic; and (b) the treatments were not very effective in the patients tested.

On the basis of our results, we hypothesize that the effectiveness of treatments with these cytokines is likely dependent on whether the tumors express low MHC class I and induce anergy of NK cells within the tumor. We found that NK cell anergy was induced specifically by MHC class I–deficient tumor cells, and could be reversed by inflammatory cytokines such as IL-12+IL-18 or H9 superkine, in line with this prediction. Conversely, we predict that the inflammatory cytokines will be markedly less effective in the case of MHC class I^+ tumors, on the basis of our findings that no anergy was induced in such tumors, and cytokine treatments had no effect in improving survival of mice with such tumors. Presumably, this can be explained, at least in part, by the relatively low sensitivity of MHC class I^+ tumors to NK-mediated killing.

Indeed, the therapeutic effects accompanying injection of inflammatory cytokines in mice bearing MHC class I–deficient tumors were striking. Notably, tumor-bearing mice treated with IL-12+IL-18 or with H9 did not exhibit differences in weight loss or body temperature compared with the untreated mice (data not shown), suggesting minimal toxicity of the cytokine treatments. As hypothesized, the longer survival of the mice injected with cytokines was correlated with restored responsiveness of intratumoral

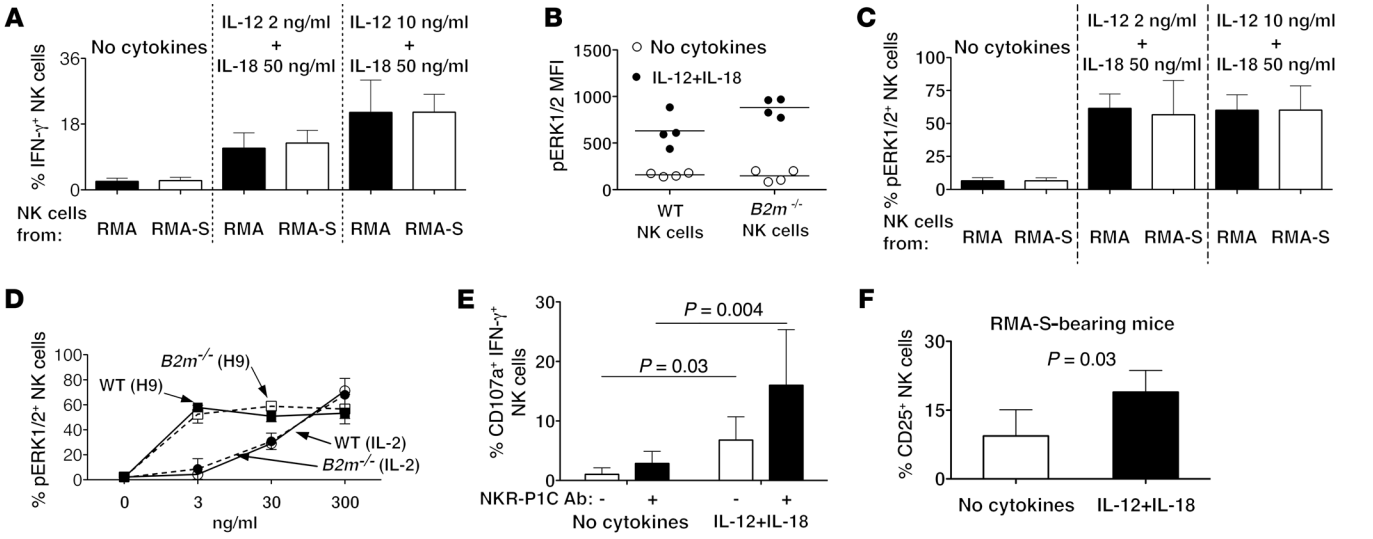

Figure 9. IL-12 and IL-18 treatment restores responsiveness in anergic NK cells. (**A**) Cells obtained from RMA or RMA-S tumors were restimulated in vitro with 2 doses of IL-18 and IL-12 for 5 hours before accumulation of IFN-γ on NK cells was assessed by flow cytometry. (**B**) Splenic cells from WT or *B2m*$^{-/-}$*Ncr1*$^{+/gfp}$ mice were stimulated for 30 minutes with no cytokines or with 50 ng/ml of IL-18 plus 10 ng/ml of IL-12 before ERK1/2 phosphorylation was assessed by flow cytometry. (**C**) Cells obtained from RMA or RMA-S tumors implanted in *Ncr1*$^{+/gfp}$ mice were stimulated for 30 minutes with the indicated doses of IL-18+IL-12, and pERK1/2 was analyzed by flow cytometry. (**D**) Splenic cells from WT or *B2m*$^{-/-}$*Ncr1*$^{+/gfp}$ mice were stimulated for 30 minutes with the indicated doses of IL-2 or H9, and pERK1/2 was analyzed by flow cytometry. (**E** and **F**) Thirteen days after injection of RMA-S cells, mice were treated or not with 100 ng each of IL-12 and IL-18, and the responsiveness of tumor-infiltrating NK cells (**E**) was assessed as described in the legend to Figure 3. Expression of CD25 (**F**) was determined by flow cytometry. In **A**, **E**, and **F**, NK cells were gated as indicated in the legend to Figure 3, whereas in **B**–**D**, NK cells were GFP$^+$. Bars represent means ± SD. The experiments included at least 4 mice per group and were performed 3 times with similar results. Statistical analyses were performed with the unpaired Student's *t* test.

NK cells. Cytokines such as IL-2 are known to restore responsiveness in anergic NK cells after in vitro culture (18, 19), but this issue has not been addressed previously in tumor models. Furthermore, the inflammatory state accompanying infections with *Listeria monocytogenes* increased the responsiveness of hyporesponsive NK subsets in normal mice (18). Most notably, cytomegalovirus infection can break tolerance to MHC class I–deficient cells in vivo (42), suggesting that inflammation contributes in determining NK cell tolerance to MHC class I–deficient cells. Our results suggest that the RMA-S tumors fail to generate adequate inflammation to reverse or prevent NK cell anergy. Notably, we failed to detect *Il12* or *Il18* mRNA within the tumors. These results fit with the hypothesis that sustained NK responses depend not only on whether the target cells display NK cell–activating ligands, but also on the inflammatory context accompanying the response. According to this proposal, infections that cause inflammation tend to sustain a long-term and effective NK cell response, whereas the relatively noninflammatory conditions within many tumors cause a more transient NK response that gradually subsides as anergy is imposed. This transient response may decrease the effectiveness of NK cells against MHC class I–deficient tumors, but it may have the benefit of limiting the capacity of NK cells to mediate inflammatory diseases when activating ligands are inappropriately expressed in tissues.

The efficacy of IL-12+IL-18 or H9 treatment in mice with RMA-S tumors raises the possibility that the enhancement of NK responses by these or other NK-activating cytokines will provide benefit to cohorts of patients with specific types of tumors, especially MHC class I–deficient tumors. Consistent with our findings, IL-12 enhanced the NK-mediated rejection of "intermediate," but not "high," doses of RMA-S cells (43), and NK cells contributed to rejection of IL-12–producing MHC class I–deficient cell lines (44). Moreover, H9 has been reported to increase the rejection of B16F10 (13), a tumor cell line reported to be an NK cell target, but which also can be rejected by T cells. In the present report, IL-12+IL-18 or H9 reversed the anergic state of NK cells infiltrating MHC class I–deficient tumors, providing a substantial therapeutic effect. We propose that the enhanced responsiveness the activating cytokines confer may provide therapeutic benefit when applied in conjunction with other agents that enhance NK cell activation, such as antibodies used for antibody-dependent cellular cytotoxicity or agents that enhance T cell responses against tumors, such as ipilimumab or antibodies that block PD-1 or its ligands. Finally, for the first time, we propose the necessity for patient stratification in order to increase the efficacy of cytokine treatment.

Our findings are likely of especially high significance for efforts to treat cancer with antibodies that block inhibitory KIR on NK cells (45–47). Such an antibody, called lirilumab (IPH2101), is currently in clinical trials for several forms of cancer. In a recent phase I trial, Vey and colleagues treated acute myeloid leukemia patients in remission with lirilumab. The treatments increased the activation of NK cells and resulted in a significant increase in overall survival (48). These results are promising, but given our results, blocking of inhibitory receptors on NK cells is likely to eventually cause anergy. On the other hand, we have also provided evidence that such anergy may be reversed by treatment with activating cytokines. Hence, our results suggest that the best results will be achieved by the combination of lirilumab and inflammatory cytokines.

For the first time, we documented induction of NK cell anergy in the context of an immune response in vivo to an MHC class I–deficient tumor. The anergic state was manifested as poor responsiveness of the cells when stimulated through different activating receptors or by an unrelated tumor cell line, and was associated with dampened early activation signals, specifically those mediating phosphorylation of ERK1/2. We propose that NK cell anergy occurs as a result of persistent stimulation of NK cells by MHC class I–deficient cells, as also occurs in the case of NK cells in MHC class I–deficient mice, which exhibit a similar anergy (10). Supporting this notion, mature WT NK cells transferred to MHC class I–deficient mice acquired a hyporesponsive functional state (17). The evidence presented herein showing that anergy in tumors did not occur in RMA-S tumors with restored MHC class I expression, and that it did occur in de novo engineered C1498 cell lines lacking MHC class I, argues compellingly that anergy induction was due to low MHC class I expression by the tumor cells.

In the present study, we exposed mice to relatively large inocula of MHC class I–deficient tumor cells, in an attempt to recreate a scenario where initial rejection of the cells fails. We propose that the NK cells initially attack the MHC class I–deficient tumor cells, but may eventually fail to eliminate them because of an acquired anergic state. This is supported by the observation that after injection of a mixture of MHC class I–positive and –negative cell lines, the resulting tumors showed a strong skewing toward RMA cells, indicating that many RMA-S tumor cells were indeed eliminated. Previous studies showed that RMA-S cells injected i.p. cause NK activation (49), but those analyses were done shortly after tumor cell inoculation (15, 16, 43, 49), whereas we observed reduced responsiveness only several days after injection of the tumor cells. In light of these considerations, it is interesting to consider what might happen in a naturally arising tumor undergoing presumptive selection for loss of MHC class I expression in vivo. We speculate that initially the small population of MHC class I–deficient tumor cells present in the tumor is sequestered from NK cell elimination, perhaps because of the localization of tumor-infiltrating NK cells and T cells to different sites within the tumor (50). Hence, the MHC class I–deficient tumor cells may significantly expand before encountering NK cells, and thereafter overwhelm the NK cell response, resulting in the induction of NK cell anergy.

The induction of anergy in subcutaneously transferred MHC class I–deficient lymphomas was a local phenomenon, as it pertained to the NK cells within the tumor itself or in the tumor-draining lymph node, but not to NK cells in distant organs or in MHC class I^+ tumors implanted on the opposite flank. MHC class I–deficient cells can invade and therefore induce NK anergy locally in the tumor-draining lymph nodes, but it remains possible that NK cells were rendered anergic in the tumor and then trafficked back to the draining lymph nodes.

In conclusion, we showed that the outcome of cytokine treatment of tumor-bearing mice largely depends on the level of expression of MHC class I molecules on tumor cells, and is associated with the anergic state that NK cells acquire within such tumors. For the first time, we demonstrated that NK cell anergy is caused by impaired signal transduction and that activating cytokines can restore the full functionality of NK cells and provide therapeutic benefit in this context.

Methods

Mice and in vivo procedures. C57BL/6J mice were bred from mice obtained from The Jackson Laboratory, and *Ncr1*$^{+/gfp}$ (51) and Ubi-GFP (23) mice were donated by Ofer Mandelboim (Hebrew University, Jerusalem, Israel) and Ellen Robey (University of California, Berkeley, California, USA), respectively. Mice were maintained at the University of California, Berkeley. Sex- and age-matched (6- to 10-week-old) mice were used for the experiments.

Tumor cells resuspended in 100 μl of RPMI without FCS were injected s.c. in the left flank (or in the right flank where indicated). Tumor development and growth were monitored by measurement of the size of the tumors with a caliper.

Where indicated, NK cells were depleted from mice by i.p. injection of 200 μg of PK136 mAb (specific for NKR-P1C, prepared in the laboratory) 5 days after tumor cell injection, repeated weekly for 4 weeks. Where indicated, each mouse received 100 ng of IL-12 (Peprotech) mixed with 100 ng of IL-18 (MBL International Corp.) or 20 μg of H9 superkine i.p. every other day starting 7 days after tumor injection and continuing for 4 weeks. For the kinetic experiments, tumor cells were injected s.c. in the left flank after resuspension of the cells in 100 μl of Growth Factor Reduced Matrigel (BD).

In most experiments, mice were killed 7, 10, or 14 days after tumor injection and tissues were collected in sterile conditions. Draining lymph nodes (inguinal), nondraining lymph nodes (brachial lymph nodes located distally to the flank in which the tumors were injected), and spleens were gently dissociated through a 70-μm filter, and the resulting single-cell suspensions were used for experiments. The tumors were excised after separation of the skin, cut in pieces, and dissociated using a gentleMACS Dissociator (Miltenyi). Dissociated tumors were digested in RPMI containing 200 μg/ml collagenase IV (Roche Applied Science) and 20 μg/ml DNase I (Sigma-Aldrich) at 37°C for 25 minutes. Except for experiments where leukocyte composition was analyzed, tumor samples were loaded on a mouse Lympholyte gradient (Cedarlane) and then used for experiments.

Cell culture. RMA, RMA-S, RMA-S/*Tap2*, C1498, C1498-*B2m*, and C1498-*Tap2* cells were cultured at 37°C in humidified atmosphere containing 5% CO_2 with RPMI supplemented with 10% FCS, 100 U/ml penicillin, 100 μg/ml streptomycin, 0.2 mg/ml glutamine, 10 μg/ml gentamicin sulfate, and 20 mM HEPES.

Antibodies. We used the following antibodies: from Biolegend, anti-CD3ε (clone 145-2C11), anti-CD4 (clone GK1.5), anti-CD11b (clone M1/70), anti-CD19 (clone 6D5), anti–DNAM-1 (clone TX42.1), anti-F4/80 (clone BM8), anti–IFN-γ (clone XMG1.2), anti-Ly6C (clone HK1.4), anti-Ly6G (clone 1A8), anti-Ly49A (clone YE1/48.10.6), anti-NKp46 (clone 29A1.4), anti–NKR-P1C (clone PK136), anti-Ter119 (clone TER-119), mouse IgG2b isotype control, and rat IgG2b isotype control; from eBioscience, anti-CD25 (clone PC61.5), anti-CD27 (clone 37.51), anti-CD45.1 (clone A20), anti-CD45.2 (clone 104), anti-CD107a (clone 1D4B), anti-Foxp3 (clone 150D/E4), anti-Ki67 (clone SolA15), anti-KLRG1 (clone 2F1), anti-Ly49G2 (clone LGL-1), anti–MHC class I H-2Db (clone 28.14.8), anti-NKG2A/C/E (clone 20d5), and anti-NKG2D (clone MI-6); from BD Pharmingen, anti-Ly49I (clone YLI-90); from Cell Signaling, anti–phospo-S473-AKT (clone D9E) and anti–phospho-T202/Y204-ERK1/2 (clone 197G2); from Jackson ImmunoResearch, goat anti-mouse IgG; from Invitrogen, goat anti-rabbit IgG. Anti-Ly49C (clone 4LO3311) was a kind gift from S. Lemieux, l'Institut National de la Recherche Scientifique–Institut Armand-Frappier (Laval, Quebec).

Flow cytometry. Dead cells were excluded by staining with Live-Dead fixable dead cell stain kit (Molecular Probes) following the manufacturer's instructions. Cells were then incubated for 20 minutes with 2.4G2 hybridoma supernatant (house-made) to block FcγRII/III receptors and for a further 20 minutes with fluorochrome- or biotin-conjugated specific antibodies, before washing. When necessary, an additional incubation with fluorochrome-conjugated streptavidin (Biolegend) was performed, and then the samples were used for flow cytometric analysis.

When necessary, intracellular staining was performed after extracellular staining by use of the Cytofix/Cytoperm kit (BD) or Foxp3-staining buffer set (eBioscience) according to the manufacturer's instructions.

Detection of phosphorylated intracellular proteins was performed by fixing of the stimulated cells with Cytofix/Cytoperm buffer (BD), then incubation with BD phospho-flow buffer II for 30 minutes in ice followed by an hour of incubation at room temperature with primary antibody and a second 1-hour incubation at room temperature with fluorochrome-conjugated secondary antibody.

Multicolor flow cytometry was performed with an LSRFortessa (BD), and data were analyzed with FlowJo software (Tree Star Inc.).

Ex vivo stimulation assays. Wells of flat-bottomed, high-protein-binding plates (Thermo Fisher Scientific) were coated with 5 μg of NKR-P1C antibody or 5 μg of mouse IgG2a as a control, or with 0.5 μg of NKp46 antibody or rat IgG2a as a control. 10^6 cells per well were stimulated for 5 hours in the presence of 1 μg of Golgi Plug (BD), 1 μg of Golgi Stop (BD), 100 U of recombinant human IL-2 (Roche), and CD107a mAb antibody (referred to as full-stimulation media). Some cells were stimulated with 400 nM PMA (Sigma-Aldrich) and 3.35 μM ionomycin (Sigma-Aldrich) diluted in full-stimulation media.

Cytokine stimulation was performed by incubation of the cells for 5 hours in the presence of 1 μg of Golgi Plug (BD) and 1 μg of Golgi Stop (BD) with the addition of 50 ng recombinant mouse IL-18 and 2 ng or 10 ng of recombinant mouse IL-12.

For phospho-flow experiments, cells from *Ncr1*$^{+/gfp}$ mice (51) were preincubated on ice for 30 minutes with NKR-P1C antibody or isotype-control antibody, washed, and then stimulated by cross-linking of the primary antibody at 37°C for 3 minutes with 2 μg of $F(ab')_2$ goat anti-mouse IgG in the presence of 50 U recombinant human IL-2. The 3′ time point was optimal on the basis of a pilot experiment. Alternatively, cells were stimulated at 37°C for 30 minutes with indicated doses of IL-12+IL-18, H9, or IL-2. Cells were stained for phospho-proteins as described in the *Flow cytometry* section.

In some experiments, tumor-infiltrating leukocytes were sorted from Ubi-GFP/BL6 mice using an Influx cell sorter (BD) and then stimulated with YAC-1 cells at a 10:1 E/T ratio for 5 hours in full-stimulation media.

RMA-S/Tap2 generation. A cDNA clone encoding WT mouse *Tap2* (gene ID 21335) was subcloned into the pQXCIN retroviral expression vector. The expression plasmid was amplified in DH5α bacterial cells and purified by standard Midi-prep (Qiagen). For transduction, 293 T cells were transfected with 1 μg of retroviral vector in combination with 1 μg of *Gag/Pol* and 1 μg of *Env* encoding plasmids using Lipofectamine 2000 according to the manufacturer's instructions. RMA-S cells were spin-infected (800 *g* for 2 hours at 22°C) with virus-containing supernatants in the presence of 8 μg/ml of Polybrene. MHC class I$^+$ cells were sorted 2 days later using an Influx cell sorter.

SDS-PAGE and Western blot. GFP$^+$ NK cells were sorted (with an Influx cell sorter) from *Ncr1*$^{+/gfp}$ mice that did or did not also harbor a homozygous *B2-microglobulin* mutation. 10^6 sorted cells were stimulated with plate-bound NKR-P1C antibody (PK136) in 96-well plates (flat bottom) for 10 minutes. Cells were then lysed in SDS sample buffer containing 0.2 mM Na_3VO_4, 1 mM NaF, 0.1 mM sodium pyrophosphate, and a protease inhibitor cocktail (Roche). Cell lysates were resolved by SDS-PAGE and transferred to nitrocellulose membranes. Membranes were blocked in 5% milk and incubated with pERK1/2 (T202/Y204) antibody, followed by HRP-coupled secondary antibodies. Following incubation with Western lightning chemiluminescence reagent (PerkinElmer), membranes were exposed to film and developed. For blotting of total ERK1/2, membranes were treated with stripping buffer (62.5 mM Tris [pH 6.8], 2% SDS, 0.7% β-Me) and incubated with ERK1/2 antibody.

RNA isolation, reverse transcription, and quantitative PCR. RNA from lysates of cell suspensions of whole tumors was extracted using the RNeasy Mini Kit (Qiagen), and treated with DNase I (DNA-free Kit, Invitrogen) for 25 minutes at 37°C. One microgram of RNA was reverse-transcribed using the iScript reverse transcriptase system (Bio-Rad) according to the manufacturer's instructions. Quantitative real-time PCR was performed on a CFX96 thermocycler (Bio-Rad) using SSO-Fast EvaGreen Supermix (Bio-Rad). 18S rRNA, β-actin, and GAPDH mRNA were used as references. The primers used for quantitative PCR analyses are listed in Supplemental Table 1 online.

Generation of MHC class I–deficient mutants of the C1498 cell line. Single guide (sg) RNAs targeting the first exon of the mouse *B2m* gene (sequence: AGTCGTCAGCATGGCTCGCT) or the fifth exon of the mouse *Tap2* gene (sequence: AGGTGAGTCGGGGCGATACC) were cloned into the LentiCRISPR lentiviral backbone vector, which also contains the *Cas9* gene (52). For transduction, 293T cells were transfected with 1 μg of lentiviral vector combined with 1 μg of p*VSVG* and 1 μg of *psPAX2* using Lipofectamine 2000 according to the manufacturer's instructions. C1498 cells were spin-infected (800 *g* for 2 hours at 22°C) with virus-containing supernatants in the presence of 8 μg/ml of Polybrene. MHC class I–deficient cells were sorted 4 days later using an Influx cell sorter.

ELISA. Blood from tumor-bearing and control mice was collected in the presence of heparin and spun down at 12,000 *g* for 10 minutes, and serum was collected. Tumors were dissociated as described in the *Mice and in vivo procedures* section. Sera were diluted 1:5 and tumor lysates 1:2 and used in an ELISA for detection of active TGF-β1 (Biolegend) according to the manufacturer's instructions.

Protein expression and purification. IL-2 and the IL-2 variant H9 were expressed and purified from Hi5 (*Trichoplusia ni*) cells as previously described (13). Soluble aggregates were removed by preparative size exclusion chromatography (SEC) with a Superdex S75. Endotoxin removal after SEC was accomplished by an additional Ni-NTA purification step accompanied by extensive column washing with 0.1% Triton X-114 prior to elution (53). Eluted proteins were desalted into PBS using PD-10 desalting columns, flash frozen in liquid nitrogen, and stored at –80°C.

Statistics. Statistical analysis was performed with the 2-tailed unpaired (or paired when indicated) Student's *t* test. Survival experiments were analyzed with the Kaplan-Maier test. For all experiments, *P* values less than 0.05 were considered statistically significant.

Study approval. All the experiments were approved by the Animal Care and Use Committee at the University of California, Berkeley, in accordance with the guidelines of the NIH.

Acknowledgments

We thank Hector Nolla and Alma Valeros for help with flow cytometry; Raulet lab members for useful discussions; Francesco Spallotta and Chiara Cencioni for help with cloning; and Giuseppe Sciume for help with phospho-flow cytometry. M. Ardolino was supported by an Istituto Pasteur-Fondazione Cenci Bolognetti postdoctoral fellowship, and by a Cancer Research Institute Irvington Fellowship. C.S. Azimi was supported by a summer undergraduate research fellowship from Rose Hill. A. Iannello holds a Special Fellow Award from the Leukemia and Lymphoma Society. W. Deng was supported by a Cancer Research Institute Irvington Fellowship. This work was supported by NIH grant R01-AI039642 and California Institute for Regenerative Medicine grant RM1-01730 to D.H. Raulet.

Address correspondence to: David H. Raulet, University of California, Berkeley, Molecular and Cell Biology, 485 LSA, Berkeley, California 94720, USA. Phone: 510.642.9521; E-mail: raulet@berkeley.edu.

1. Margolin K. Cytokine therapy in cancer. *Expert Opin Biol Ther*. 2008;8(10):1495–1505.
2. Atkins MB, Regan M, McDermott D. Update on the role of interleukin 2 and other cytokines in the treatment of patients with stage IV renal carcinoma. *Clin Cancer Res*. 2004; 10(18 pt 2):6342S–6346S.
3. Coughlin CM, et al. Interleukin-12 and interleukin-18 synergistically induce murine tumor regression which involves inhibition of angiogenesis. *J Clin Invest*. 1998;101(6):1441–1452.
4. Yoshimoto T, Nagai N, Ohkusu K, Ueda H, Okamura H, Nakanishi K. LPS-stimulated SJL macrophages produce IL-12 and IL-18 that inhibit IgE production in vitro by induction of IFN-γ production from CD3intIL-2R β+ T cells. *J Immunol*. 1998;161(3):1483–1492.
5. Yoshimoto T, et al. IL-12 up-regulates IL-18 receptor expression on T cells, Th1 cells, and B cells: synergism with IL-18 for IFN-γ production. *J Immunol*. 1998;161(7):3400–3407.
6. Kaufman HL, Flanagan K, Lee CS, Perretta DJ, Horig H. Insertion of interleukin-2 (IL-2) and interleukin-12 (IL-12) genes into vaccinia virus results in effective anti-tumor responses without toxicity. *Vaccine*. 2002;20(13–14):1862–1869.
7. Li Q, et al. Synergistic effects of IL-12 and IL-18 in skewing tumor-reactive T-cell responses towards a type 1 pattern. *Cancer Res*. 2005;65(3):1063–1070.
8. Vivier E, Ugolini S, Blaise D, Chabannon C, Brossay L. Targeting natural killer cells and natural killer T cells in cancer. *Nat Rev Immunol*. 2012;12(4):239–252.
9. Joncker NT, Raulet DH. Regulation of NK cell responsiveness to achieve self-tolerance and maximal responses to diseased target cells. *Immunol Rev*. 2008;224:85–97.
10. Shifrin N, Raulet DH, Ardolino M. NK cell self tolerance, responsiveness and missing self recognition. *Semin Immunol*. 2014;26(2):138–144.
11. Raulet DH, Vance RE. Self-tolerance of natural killer cells. *Nat Rev Immunol*. 2006;6(7):520–531.
12. Garrido F, Algarra I. MHC antigens and tumor escape from immune surveillance. *Adv Cancer Res*. 2001;83:117–158.
13. Levin AM, et al. Exploiting a natural conformational switch to engineer an interleukin-2 'superkine'. *Nature*. 2012;484(7395):529–533.
14. Ljunggren HG, Karre K. Host resistance directed selectively against H-2-deficient lymphoma variants. Analysis of the mechanism. *J Exp Med*. 1985;162(6):1745–1759.
15. Karre K, Ljunggren HG, Piontek G, Kiessling R. Selective rejection of H-2-deficient lymphoma variants suggests alternative immune defence strategy. *Nature*. 1986;319(6055):675–678.
16. Diefenbach A, Jensen ER, Jamieson AM, Raulet DH. Rae1 and H60 ligands of the NKG2D receptor stimulate tumour immunity. *Nature*. 2001;413(6852):165–171.
17. Joncker NT, Shifrin N, Delebecque F, Raulet DH. Mature natural killer cells reset their responsiveness when exposed to an altered MHC environment. *J Exp Med*. 2010;207(10):2065–2072.
18. Fernandez NC, Treiner E, Vance RE, Jamieson AM, Lemieux S, Raulet DH. A subset of natural killer cells achieves self-tolerance without expressing inhibitory receptors specific for self-MHC molecules. *Blood*. 2005;105(11):4416–4423.
19. Kim S, et al. Licensing of natural killer cells by host major histocompatibility complex class I molecules. *Nature*. 2005;436(7051):709–713.
20. Attaya M, et al. Ham-2 corrects the class I antigen-processing defect in RMA-S cells. *Nature*. 1992;355(6361):647–649.
21. Yang Y, et al. Major histocompatibility complex (MHC)-encoded HAM2 is necessary for antigenic peptide loading onto class I MHC molecules. *J Biol Chem*. 1992;267(17):11669–11672.
22. Benton G, Kleinman HK, George J, Arnaoutova I. Multiple uses of basement membrane-like matrix (BME/Matrigel) in vitro and in vivo with cancer cells. *Int J Cancer*. 2011;128(8):1751–1757.
23. Schaefer BC, Schaefer ML, Kappler JW, Marrack P, Kedl RM. Observation of antigen-dependent CD8+ T-cell/dendritic cell interactions in vivo. *Cell Immunol*. 2001;214(2):110–122.
24. Jinek M, Chylinski K, Fonfara I, Hauer M, Doudna JA, Charpentier E. A programmable dual-RNA-guided DNA endonuclease in adaptive bacterial immunity. *Science*. 2012;337(6096):816–821.
25. Sander JD, Joung JK. CRISPR-Cas systems for editing, regulating and targeting genomes. *Nat Biotechnol*. 2014;32(4):347–355.
26. LaBelle JL, Truitt RL. Characterization of a murine NKT cell tumor previously described as an acute myelogenous leukemia. *Leuk Lymphoma*. 2002;43(8):1637–1644.
27. Bix M, Liao NS, Zijlstra M, Loring J, Jaenisch R, Raulet D. Rejection of class I MHC-deficient haemopoietic cells by irradiated MHC-matched mice. *Nature*. 1991;349(6307):329–331.
28. Liao N, Bix M, Zijlstra M, Jaenisch R, Raulet D. MHC class I deficiency: susceptibility to natural killer (NK) cells and impaired NK activity. *Science*. 1991;253(5016):199–202.
29. Wei S, et al. Control of lytic function by mitogen-activated protein kinase/extracellular regulatory kinase 2 (ERK2) in a human natural killer cell line: identification of perforin and granzyme B mobilization by functional ERK2. *J Exp Med*. 1998;187(11):1753–1765.
30. Vivier E, Nunes JA, Vely F. Natural killer cell signaling pathways. *Science*. 2004;306(5701):1517–1519.
31. Roux PP, Blenis J. ERK and p38 MAPK-activated protein kinases: a family of protein kinases with diverse biological functions. *Microbiol Mol Biol Rev*. 2004;68(2):320–344.
32. Chiossone L, Chaix J, Fuseri N, Roth C, Vivier E, Walzer T. Maturation of mouse NK cells is a 4-stage developmental program. *Blood*. 2009;113(22):5488–5496.
33. Joncker NT, Fernandez NC, Treiner E, Vivier E, Raulet DH. NK cell responsiveness is tuned commensurate with the number of inhibitory receptors for self-MHC class I: the rheostat model. *J Immunol*. 2009;182(8):4572–4580.
34. Ghiringhelli F, Menard C, Martin F, Zitvogel L. The role of regulatory T cells in the control of natural killer cells: relevance during tumor progression. *Immunol Rev*. 2006;214:229–238.
35. Hoechst B, et al. Myeloid derived suppressor cells inhibit natural killer cells in patients with hepatocellular carcinoma via the NKp30 receptor. *Hepatology*. 2009;50(3):799–807.
36. Li H, Han Y, Guo Q, Zhang M, Cao X. Cancer-expanded myeloid-derived suppressor cells induce anergy of NK cells through membrane-bound TGF-beta 1. *J Immunol*. 2009;182(1):240–249.
37. Hong H, et al. Depletion of $CD4^+CD25^+$ regulatory T cells enhances natural killer T cell-mediated anti-tumour immunity in a murine mammary breast cancer model. *Clin Exp Immunol*. 2010;159(1):93–99.
38. Srivastava MK, et al. Myeloid suppressor cell depletion augments antitumor activity in lung cancer. *PLoS One*. 2012;7(7):e40677.
39. Gill S, et al. Tate K, Ritchie DS, et al. Rapid development of exhaustion and down-regulation of eomesodermin limit the antitumor activity of adoptively transferred murine natural killer cells. *Blood*. 2012;119(24):5758–5768.
40. Ni J, Miller M, Stojanovic A, Garbi N, Cerwenka A. Sustained effector function of IL-12/15/18-preactivated NK cells against established tumors. *J Exp Med*. 2012;209(13):2351–2365.
41. Pardoll DM. The blockade of immune checkpoints in cancer immunotherapy. *Nat Rev Cancer*. 2012;12(4):252–264.
42. Sun JC, Lanier LL. Cutting edge: viral infection breaks NK cell tolerance to "missing self". *J Immunol*. 2008;181(11):7453–7457.
43. Grufman P, Karre K. Innate and adaptive immunity to tumors: IL-12 is required for optimal responses.

Eur J Immunol. 2000;30(4):1088–1093.
44. Nanni P, et al. Interleukin 12 gene therapy of MHC-negative murine melanoma metastases. *Cancer Res*. 1998;58(6):1225–1230.
45. Romagne F, et al. Preclinical characterization of 1-7F9, a novel human anti-KIR receptor therapeutic antibody that augments natural killer-mediated killing of tumor cells. *Blood*. 2009;114(13):2667–2677.
46. Sola C, et al. Genetic and antibody-mediated reprogramming of natural killer cell missing-self recognition in vivo. *Proc Natl Acad Sci U S A*. 2009;106(31):12879–12884.
47. Vahlne G, et al. In vivo tumor cell rejection induced by NK cell inhibitory receptor blockade: maintained tolerance to normal cells even in the presence of IL-2. *Eur J Immunol*. 2010;40(3):813–823.
48. Vey N, et al. A phase I trial of the anti-inhibitory KIR monoclonal antibody IPH2101 for acute myeloid leukemia (AML) in complete remission. *Blood*. 2012;120(22):4317–4323.
49. Glas R, et al. Recruitment and activation of natural killer (NK) cells in vivo determined by the target cell phenotype. An adaptive component of NK cell-mediated responses. *J Exp Med*. 2000;191(1):129–138.
50. Deguine J, Breart B, Lemaitre F, Di Santo JP, Bousso P. Intravital imaging reveals distinct dynamics for natural killer and CD8(+) T cells during tumor regression. *Immunity*. 2010;33(4):632–644.
51. Gazit R, et al. Lethal influenza infection in the absence of the natural killer cell receptor gene Ncr1. *Nat Immunol*. 2006;7(5):517–523.
52. Shalem O, et al. Genome-scale CRISPR-Cas9 knockout screening in human cells. *Science*. 2014;343(6166):84–87.
53. Reichelt P, Schwarz C, Donzeau M. Single step protocol to purify recombinant proteins with low endotoxin contents. *Protein Expr Purif*. 2006;46(2):483–488.